

24 Interferometry with Macromolecules: Quantum Paradigms Tested in the Mesoscopic World

Markus Arndt, Olaf Nairz, Anton Zeilinger

24.1 A Prototype Quantum Experiment

When thinking about quantum non-locality a modern physicist would probably think of two-particle entanglement first. And many beautiful experimental demonstrations have been published on quantum systems which violate Bell's inequalities [1].

However non-locality as well as almost all other quantum 'mysteries' can be found in even simpler experiments as we will discuss in the context of single-particle interferometry of large molecules. This is why *Feynman* et al called the double-slit experiment the heart of quantum mechanics [2]. And this is also the reason why the exploration of interference effects with more massive and complex, mesoscopic systems will also help us elucidate important features of physics along the quantum–classical boundary.

Imagine first a classical soccer player aiming with a ball at a wall with a single opening, as sketched in Fig. 24.1a. If we further assume an infinitely thin wall with a slit which is just wide enough to let the ball pass then we would expect only a single point in the goal to be hit by a few balls. All the other points in the goal will be masked by the wall. If we open the gap in the wall and allow for wall thickness then we would expect different balls to hit the goal at different places, both because the player may kick different balls differently and because there may be scattering at the wall edges. Classically we would therefore expect a certain position distribution.

In contrast to that, what would be the result in a quantum version of the game? There we can use an argument based on the *Heisenberg* uncertainty relation [3]. The passage through the hole in the wall improves the knowledge of the position state of the ball. Given the complementarity between position and momentum we conclude that the momentum uncertainty after the wall must be larger than before. In the plane of the goal this translates into a spread of the possible ball positions. Narrowing the wall opening will therefore narrow the position distribution for classical balls but widen the corresponding quantum distribution. The same description obviously holds also for the case where we open the right door in the wall instead of the left one, as sketched in Fig. 24.1b.

If we now open both doors a classical physicist will simply expect the two probability distributions for two single openings to add up to a big hump.

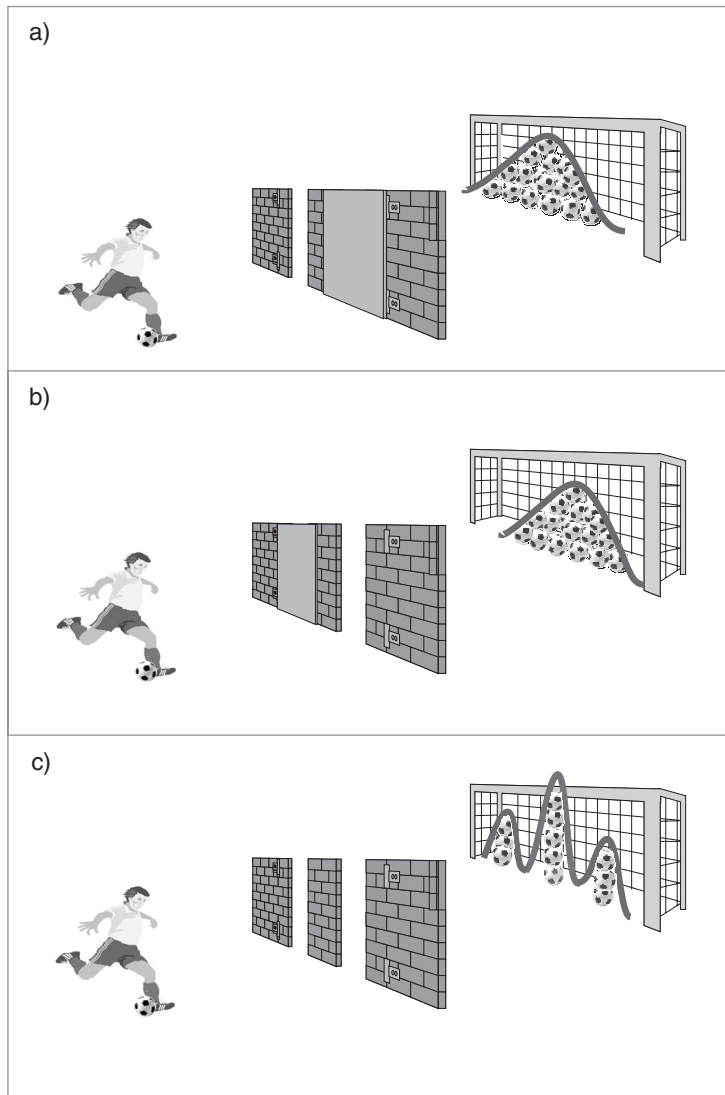


Fig. 24.1. Wave particle duality: a quantum paradigm confronted with our everyday experience

She will expect that at any point in the goal the number of balls can only grow when we open the second door. This is the experience made when using real soccer balls in real life.

However, under appropriate quantum circumstances the observer can actually see a pattern which differs dramatically from this expectation. *Opening* the second door *can dramatically reduce* the number of balls hitting the goal

in specific places. In particular one can find well-defined places which will be completely avoided by all balls, as sketched in Fig. 24.1c.

A classical model which helps in understanding a part of the phenomenon is the wave picture: If we regard each ball as a wave illuminating the two openings simultaneously then we actually expect to see interference of the wavelets if they take *indistinguishable paths* through the slits in the wall.

While we usually accept this explanation for water waves, we run into trouble when we shoot one ball at a time: How can a commonly *well-localized object*, i.e. a *particle* like a ball, acquire *non-local* information about widely separated wall openings, as we accept the situation to be for a *wave*? In addition, if the ball is a non-local object with *position uncertainty* at the wall openings, how can it decide upon its final well-localized position in the goal? What actually is the famous *collapse* of the wave function? All experiments so far are consistent with the view that each particle chooses its final location on the screen *randomly*, although the total ensemble will finally generate an interference pattern which is completely *deterministic*. How can this be understood?

In summary, we find at least the following quantum notions in the context of double-slit interferometry: complementarity, uncertainty, non-locality, superposition of classically exclusive states, wave-particle duality, objective randomness and the collapse of the wave function. All of these ‘mysteries’ may be subsumed by the notion that quantum mechanics describes potentiality instead of reality. It is important to note that potentiality is often the only objective reality.

Finally, another key ingredient of quantum physics has to be mentioned: entanglement, the inseparable correlation of at least two quantum systems – which can also be part of the same physical object, as in the entanglement of internal and external degrees of freedom. This property will become relevant in the context of decoherence, as discussed further below. In the double-slit experiment the degree of entanglement between system and environment is actually important for the possibility of observing either the particle or the wave nature.

All these quantum effects have been known for more than 70 years, but even though we have learnt to accept their weirdness, there remain many open questions. Two of them are at the origin of the present work: Firstly, how can we understand the transition from the quantum to the classical world? In our classical world we see neither objective randomness nor spontaneous collapses nor wave effects of macroscopic objects nor quantum correlations between space-like-separated objects. Under which circumstances and at which scale do these properties disappear? Secondly, can we arrange experiments such that we observe and possibly exploit quantum phenomena on the mesoscopic or even macroscopic scale?

24.2 Interference of Fullerenes

While the discussion of classical soccer balls in the introduction appears somewhat academic, since we cannot see quantum effects for them, we can construct an experiment in which we may gradually approach the transition from the quantum to the classical case. Our experiment is based on the world's smallest soccer balls, composed of 60 carbon atoms.

Most quantum interference experiments so far have dealt with microscopic objects, such as electrons [4], neutrons [5, 6] and atoms [7] or, more recently, with coherent ensembles of ultra-cold atoms [8]. Complementary to that, our studies investigate strongly bound hot particles which form a mesoscopic single quantum object. Our experiments are in a parameter regime unexplored hitherto and may allow the investigation of the quantum–classical transition in complex systems.

Fullerenes, in particular C_{60} and C_{70} , turned out to be very good candidates for studies on the route towards the mesoscopic world. They represent a qualitative step forward with respect to previous experiments, since these carbon cages resemble in many aspects rather classical lumps of carbon than simple quantum systems. They have more than 100 different vibrational modes, leading to broad optical lines, highly excited rotational states and both non-radiative and radiative transitions between most of them. Because of the rapid thermalization it is possible to assign a temperature to the internal energy distribution. Moreover, as for macro-objects, one experimentally finds both line radiation, from vibrational transitions, and a continuous blackbody spectrum as well as thermal electron emission [10, 11]. It is this internal complexity and energy which is new and which may give rise to new phenomena. Also, from a practical point of view, fullerenes are the macromolecules of choice, since they are available in a sufficient amount, can be sublimated to produce a thermal beam and have the required symmetry and stability to survive their time in the vacuum machine without significant fragmentation.

The setup of the fullerene interference experiments is as sketched in Fig. 24.2 and has been described in more detail in [9, 12]. Fullerenes are sublimated and collimated. Depending on the performed experiment, they are either diffracted at the second slit or at a nanofabricated grating immediately behind this slit. The Fraunhofer far-field interference pattern is subsequently scanned with well-focused intense visible laser light, which thermally ionizes the fullerenes. In the following figures the ion count rate is plotted as a function of the detection-laser position.

Since the experiment is based on a thermal source, i.e. a classical mixture of external and internal molecule states, one may wonder why interference is possible at all. In the elementary introduction to double-slit interferometry we emphasized that the indistinguishability of all possible paths is an essential requirement for interference. It is important to note that each molecule is very likely to be in a state completely different to that of any other particle in the

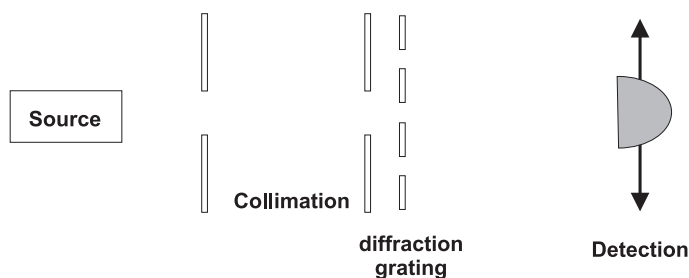


Fig. 24.2. Simplified setup of the fullerene interference experiment [9]. Fullerenes are sublimated and collimated. They are either diffracted at the second slit or at a nanofabricated grating immediately behind this slit. The Fraunhofer far-field interference pattern is subsequently scanned with a scanning laser. The laser thermally ionizes the fullerenes. In the following figures this ion count rate is plotted as a function of the detection-laser position. For the single-slit interference of Fig. 24.3 the grating is taken out and the width of slit 2 can be varied between 70 and 20 000 nm. For the diffraction-grating experiments the second slit is fixed at 5 μm and the grating is shifted into the beam

thermal ensemble. We can therefore expect to observe only the interference of each molecule with itself. In order to obtain good contrast one has therefore to restrict the initial momentum and position distribution. This then provides the required spectral and spatial coherence of the interfering waves.

A wide *velocity distribution* generally results in a poor *spectral coherence*. Molecules at different speeds have different diffraction angles. Since their interference patterns add incoherently on the screen, they tend to wash out.

The *spatial coherence* is the second important aspect in the preparation of the beam. Within the source the fullerenes can be regarded as very well localized, in general, to a width corresponding to their thermal de Broglie wavelength [14]. This is of the order of a few picometers and thus more than 100 times smaller than the diameter of C_{60} . This is why the notion of a particle is well justified while the particle is in the oven. However, as the molecules fly freely towards the grating, their wave function is spreading out. The transverse coherence width at the grating can then be regarded as being roughly the width of the zeroth-order peak due to diffraction at the first collimation slit [15]. In the grating interference experiments this transverse coherence width amounts to about 1 μm .

That *single-slit diffraction* actually takes place even for the hot and heavy molecule C_{70} is demonstrated in Fig. 24.3. For this figure the width of the second collimation slit was gradually closed from 18.6 μm in Fig. 24.3a via 1.4 μm in Fig. 24.3b down to 70 nm in Fig. 24.3c, and the far field molecular beam width was recorded. While the beam width is actually composed of several contributions – including the detector resolution and the classical collimation – it is evident that for small slit widths the Heisenberg uncertainty relation between position and momentum must become relevant. This

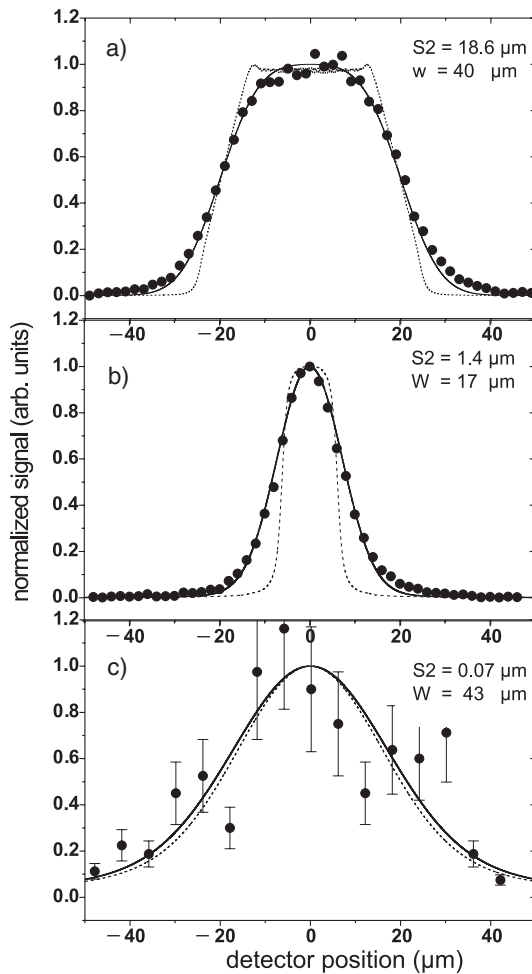


Fig. 24.3. Single-slit diffraction for C_{70} . (a–c) A decreasing width of the second slit. The far-field molecular beam pattern reflects the broadening of the momentum distribution in agreement with Heisenberg’s uncertainty relation. See also [13]

qualitative evolution can be seen in Fig. 24.3a–c where the observed molecular beam changes its width (FWHM) from $\Delta X_{\text{mol}} = 40 \mu\text{m}$ via $\Delta X_{\text{mol}} = 17 \mu\text{m}$ to $W = 43 \mu\text{m}$. It can clearly be seen that, when the collimation is improved, the molecular beam first becomes narrower and then spreads out again. In [13] we have shown that this effect is not only in qualitative but also in good quantitative agreement with expectations from a wave calculation for the Heisenberg uncertainty relation.

Based on this experiment we know that diffraction at a 70-nm-wide gap leads to an angular spread of the beam of more than $\sim 33 \mu\text{rad}$. We now

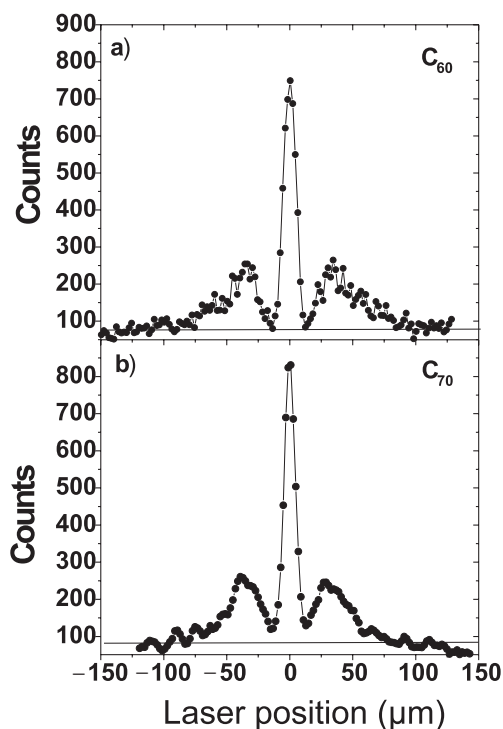


Fig. 24.4. High-contrast interference for C_{60} and C_{70} . For this picture the collimation was set to its optimum value, limited by diffraction at the second collimation slit [18]. Minima are a signature of destructive interference. In the curves presented here the minimum goes to the background level, indicating almost 100% interference contrast, in spite of the high internal excitation and a non-vanishing probability for internal state changes during the passage from the grating to the detector

ask if this spread is sufficiently coherent for high-contrast interference fringes after diffraction at a grating. In order to test this we look for the key feature of grating interference, namely the complete extinction of the probability amplitude at certain positions on the screen due to destructive interference. The setup is as above, but complemented by a nanofabricated SiN structure close behind the second collimation slit. Many slits are each etched ~ 50 nm wide and into the 200-nm-thick SiN membrane¹ to form a grating with a period of 100 nm. About 20–30 such slits are illuminated by the molecular beam. The coherence width covers about 10 such slits. Figure 24.4a,b shows interference patterns for thermal beams of C_{60} and C_{70} respectively. In both cases one can clearly recognize the first-order interference maxima and minima. The absence of higher orders of diffraction is due to the broad spectral width of

¹ Gratings were provided by H. Smith and T. Savas, MIT, Cambridge, Mass. The manufacturing technology is described in [16].

the molecule source as can also be found in a numerical model.² In spite of this limitation, the interference minimum approaches the background count rate. This high interference contrast is a clear proof of nearly perfect coherence.

24.3 Decoherence

The de Broglie wavelength is in principle a well-defined concept for any object of arbitrary mass, size and complexity. One could therefore be tempted to say that the above experiments do not show anything surprising. However, in spite of being well defined, quantum interference of a chair or table is never observed.

There may be several reasons for this. On the one hand, a widespread and valid argument is the smallness of the effect. The mass of a chair is so big that at a speed of 1 m/s, i.e. the velocity of a typical pedestrian, the de Broglie wavelength of the chair is close to the Planck length of 10^{-35} m. It is clear that a superposition pattern of such wavelengths will be experimentally inaccessible. However, often quantum effects disappear well before any technological resolution limit. While several models have been put forward to complement or modify quantum physics [19, 20], we shall focus here on decoherence theory as developed in much more detail in [14, 21, 22]. This model describes the loss of correlations within a quantum system as being the result of the interaction of the system with the environment.

Any interaction of the quantum system with the outside world – be it the interaction with a conscious observer using a measuring device (a meter) or only an accidental coupling to the environment – has the effect of entangling the system with this environment. The *von Neumann* measurement of the quantum state $|\Phi_n\rangle$ turns the initial meter pointer $|\Phi_0\rangle$ into a position correlated with the quantum state $|\Phi_n\rangle$:

$$|\phi_n\rangle |\Phi_0\rangle \xrightarrow{\text{measure}} |\phi_n\rangle |\Phi_n\rangle . \quad (24.1)$$

A reliable meter is necessarily based on this correlating interaction.³ The situation becomes puzzling when the quantum system is in a superposition state. By linearity of quantum mechanics, a macroscopic superposition of meter states (pointer positions) should then also exist,

$$\left(\sum_n c_n |n\rangle \right) |\Phi_0\rangle \xrightarrow{\text{measure}} \sum_n c_n |n\rangle |\Phi_n\rangle . \quad (24.2)$$

However this phenomenon has never been observed. As has been pointed out in [21, 22], the conflict with reality can be reduced if one considers that

² Experiments with improved longitudinal coherence length show higher-order interference fringes, as shown in [17].

³ The accidental interaction with the environment does not in general act as an ideal meter. The correlation can be much weaker than indicated in (24.1).

the *entanglement* (non-separability) of the system and the meter may de facto be unobservable due to the large number of degrees of freedom of the meter. Therefore, if the experiment measures the system alone and ignores the environment, the correct answer to any experimental question will be based on a reduced density matrix which has been *traced over the meter states*. If all pointer states are sufficiently distinct, i.e. $\langle \Phi_n | \Phi_m \rangle \simeq 0$, it can be shown that the quantum system is forced into a classical mixed state, lacking all coherence and ability to interfere.

This formalism may be interpreted in a different way, too. If the corresponding environmental states are completely distinct from each other, the information about the quantum systems can be known with absolute certainty after its coupling to the environment. This rephrases, confirms and mathematically justifies Bohr's rule of complementarity that interference must disappear if we obtain definite which-path information [23].

How would this apply to our fullerene experiment? Suppose we had a UV laser with a wavelength of below ~ 100 nm. Then scattering of a laser photon by a fullerene would give us sufficient information about which way the molecule took through the diffraction grating. Therefore the environmental states would be orthogonal and the interference pattern should disappear. As a matter of fact, one can formulate even a third rule for the limit of interference: The coupling to the environment will in most cases go along with a random momentum transfer. In the described example this random recoil and corresponding phase shift of the molecular wave function is due to the scattering of the UV photons. The different phase shifts acquired by the different molecules will finally wash out the interference pattern. Purist decoherence theorists would claim that the three processes – entanglement with the environment, which-path information and phase shifts due to momentum recoil – are completely different and should not be mixed. One could be tempted to argue that a very massive object, such as a large building, could be entangled with the town and localized by a radio-wave photon without getting any measurable recoil. However, if we follow Bohr's rule that we should not talk about things that we cannot measure, then we can safely claim that all three arguments are faces of the same physics in pure de Broglie interferometers⁴; for example, in order to experimentally prove that there is coherence in the center of mass wave function of the building, one would have to repeat an interference experiment with it. Since the de Broglie wavelength and the corresponding diffraction angles after the grating would be microscopically tiny, the detection screen would have to be placed at an astronomical distance in order to resolve the diffraction orders. It turns out formally that a photon that would be sufficient to locate the building in any

⁴ The information storage and entanglement can be very different in interferometers which also exploit internal states of the quantum system. Examples of this phenomenon, emphasizing the aspect of complementarity as opposed to simple phase diffusion, are discussed in [24, 25].

given grating slit – a condition required for producing orthogonal states in the environment – would also give the random recoil required to wash out the interference pattern.

Localization and entanglement via a single strong scattering event, as discussed so far, is not the only way of producing decoherence. One can also gradually gain which-path information by many weak coupling processes. This is actually the more interesting case both from a theoretical point of view [14] and with respect to thermal decoherence. For experiments dealing with spatial superposition states, one can show that the off-diagonal matrix elements, representing the coherences, decay exponentially in time, in the squared separation of the position wave packets and in the decoherence parameter:

$$\rho(x, x', t) = \rho(x, x', 0) \exp[-\Lambda t(x - x')^2] . \quad (24.3)$$

Here the decoherence parameter is given by $\Lambda = \Gamma \cdot k^2$ [22] and is a measure for the interaction rate, Γ , and the square of the interaction strength, as defined by the wave number, k , of the particles which are scattered or emitted into the environment. Many weak scattering processes can yield sufficient entanglement, which-path information and momentum diffusion to destroy the interference pattern.

Experiments on decoherence in atom interferometers have already been performed by different groups [26–28] using the interaction of the atoms with external radiation. In contrast to that, experiments with the fullerene molecules may provide a way to look at naturally occurring *thermal decoherence* processes. Which-path information and entanglement could be produced by the fullerenes in scattering or emission processes. But also correlations of interferometric phase shifts with external fields may become important. Several of these interactions shall be discussed in the following.

24.3.1 Vibrational Transitions

At $T \sim 900$ K, as in our experiment, each C_{60} molecule has on average a total vibrational energy of $E_v \sim 5$ eV [29] stored in 174 vibrational modes at 46 different energies. *Non-radiative transitions* between many of them are in principle possible. However they are *per definitionem* decoupled from the environment. Any possible transition takes place in a superposition of all position states. One could even say that – since both the energy and entropy remain conserved – all such ‘transitions’ are actually part of a unitary and coherence-preserving transformation. The center of mass motion, the environment and the available position information are unaffected. The interference pattern must therefore remain unperturbed.

Radiative transitions are possible between electronically excited and ground states as well as among vibrational modes. In the case of C_{60} the latter are limited to four threefold degenerate vibrational modes. They emit

at $\lambda_{\text{vib}} = 7.11, 8.57, 17.54$ and $18.98 \mu\text{m}$ [30]. A single photon at these wavelengths is certainly insufficient – by about a factor of one hundred in energy – to yield unambiguous which-path information in our grating experiment.

While the wavelengths are precisely known, the values for the line strengths have been a matter of debate in the literature. The most recent values for the Einstein coefficients are of the order of $A_k \sim 2 - 30 / \text{s}$ [31]. Other authors estimate that, even if one includes combination lines and overtones for C_{60} heated to 3500 K, the total emitted vibrational energy will be below 16 eV/s, which corresponds to one or two IR photons during the 10 ms time of flight through our vacuum can [32].

The situation is slightly different for the less symmetric fullerene, C_{70} . It shows 31 different IR emission lines – out of 204 vibrational modes. Again the emission wavelengths are situated between 10 and 20 μm and thus much too long for single-photon decoherence. Experiments in our lab have shown [33] that even at the increased number of allowed transitions the number of photons is still insufficient to induce a sizable loss of contrast.

It is interesting to ask how internal properties will affect the interference of larger objects. It may be assumed that with increasing complexity also the number of allowed transitions will increase and therefore the ability to diffuse quantum coherence into the environment. However, one should also consider that a minimum energy of $\sim 0.1 \text{ eV}$ is generally required for the excitation of a vibrational level. Substantial cooling of the internal degrees of freedom seems to be within the reach of current technologies even for macromolecules using jet expansion or buffer gas techniques [34]. Exploitation of these methods should render coherence experiments feasible.

24.3.2 Emission of Blackbody Radiation

Laser-heated C_{60} has been observed [10, 35] to emit blackbody radiation with a continuous spectrum in functional agreement with Planck's radiation law corrected by the factor $8\pi R/\lambda$. This factor takes into account that the radius, R , of a fullerene is much smaller than the emitted wavelength, λ [36]. The 'black' body therefore radiates rather in bright grey. A wavelength-integrated emissivity of $\varepsilon \sim (4.5 \pm 2.0) \times 10^{-5}$ has been published in [29]. From this value we can derive an upper bound on the energy that can be lost while the buckyball is flying from the grating to the detector. For a typical value of $T \sim 900 \text{ K}$ the average energy emitted during the time of flight can be estimated to be $E_{\text{bb}} \sim 0.1 \text{ eV}$. This corresponds to the energy of a single photon at $\lambda \sim 10 \mu\text{m}$. A natural question arises as to whether it is possible to increase the temperature to see a gradual increase in radiation and decoherence. Using our detection light, derived from an argon ion laser we can easily increase the molecular energy up to 40 eV. The maximal energy that can be stored in the molecule is limited by the onset of fragmentation or ionization on the 10–100 μs time scale for temperatures higher than 3000 K (corresponding to $E_{\text{int}} = 37 \text{ eV}$ [10]). At a thus threefold-increased temperature we

would expect an 81-fold increase in black body-emission intensity. This should already give rise to a measurable phase diffusion. Since many macromolecular parameters are very difficult to access experimentally and because of the sizeable uncertainty for many values published in the literature, we have implemented laser heating for the fullerenes and searched for a broadening of the molecular beam or a decrease in the contrast of the interference pattern. In all preliminary experiments performed so far the contrast in the presence of laser heating was always comparable to the case when we used a thermal beam source alone. We therefore conclude that blackbody emission is still too weak in our present experiments in spite of the high internal temperatures.

However, we expect that for much larger particles than the fullerenes this will change significantly. The emitted intensity scales with the third power of the particle size, R^3 , both because of the increasing surface (R^2) and because of the antenna effect (R/λ) mentioned above. For particles in the ‘30 nm’ region, corresponding to the size of a small virus or a medium nanocrystal, it will therefore be necessary to lower the internal temperature to below $T \sim 30$ K. The generation of sufficiently intense beams of particles having this size and temperature is certainly non-trivial. But we believe that it is still within the reach of the emerging technologies.

24.3.3 Absorption of Blackbody Radiation

In our fullerene experiments absorption of blackbody radiation has a smaller influence on decoherence than any emission, since the environment is at a much lower temperature than the fullerene molecule. This changes when we consider larger objects. A billiard ball will certainly absorb enough blackbody photons to decohere more rapidly than we can perform a room temperature interference experiment with it. However, up to at least the size of a small virus we expect that the detrimental effect of blackbody absorption can be suppressed under moderate cryogenic conditions.

24.3.4 Rayleigh Scattering of Thermal Radiation

Here we treat the case of a particle of dielectric constant ϵ and radius a which is bombarded by thermal radiation at temperature T . For this particular situation *Joos* et al. have calculated the decoherence parameter of (24.3) due to Rayleigh scattering to be [22]:

$$A[\text{m}^{-2}\text{s}^{-1}] \sim 10^{36} \cdot a^6 \cdot T^9 \cdot \left(\frac{\epsilon - 1}{\epsilon + 1} \right)^2 . \quad (24.4)$$

To obtain a rough estimate for the importance of this effect, let us assume that the typical time of flight through our interferometer is 10 ms for the currently used buckyballs and 0.9 s for a virus beam of mass 10^7 amu at a velocity of 4.4 m/s. The latter speed is chosen to yield a vertical parabola

of 1 m height. It turns out that Rayleigh scattering of 300 K blackbody radiation limits the maximal coherent wave packet separation of the buckyball to 1 m! The dielectric constants of most macromolecules are unknown. For an order of magnitude estimate we therefore use the bulk dielectric constant of water, $\epsilon = 80$, and the radius of a small virus, say 15 nm. For such a water cluster the largest possible coherent separation would already be limited to $\Delta x_{\text{coh}} < 2.3 \mu\text{m}$, which is small but still an order of magnitude larger than the beam splitting in a reasonable near-field interferometer. For objects with a higher dielectric constant or a larger diameter, the dramatic size dependence in (24.4) can in principle be counteracted by a significant reduction of the temperature of the vacuum machine.

24.3.5 Fragmentation and Ionization

The emission of either C_2 subunits or electrons, is a possible process in fullerene interferometry at high temperatures. However, it only becomes relevant at temperatures around 3000 K. Moreover both would rather contribute to a loss of molecules than to decoherence, since the imparted recoil would be sufficient to kick the molecules beyond the detection region. Most biological macromolecules are much more thermo-labile than C_{60} . Even at moderate temperatures configuration changes and fragmentation are likely. But anyway a realistic interference experiment would have to be performed at low molecule temperatures for the reasons given above.

24.3.6 Influence of Collisions with the Residual Gas

Collisions with gas molecules are in principle very effective in determining positions and destroying coherence. This is due to the very small de Broglie wavelength of the fast nitrogen or oxygen molecules. Several authors [22] therefore claim that even at the best possible laboratory vacuum, decoherence must be very fast. We argue in this section that the perturbative approach to decoherence theory does actually not apply to our experiment, although the computed decoherence parameters are correct. As described earlier, the decoherence parameter, Λ , of (24.3) is the product of a scattering rate, Γ , and the square of the wave number, k^2 , of the incident molecule. While the first is generally small the momentum transfer is generally much too strong to allow the application of perturbation theory.

As a matter of fact the influence of collisions on the observability of the interference fringes depends on the setup of the experiment. Since small angle collisions have a much higher scattering cross-section than wide-angle collisions, far-field diffraction patterns with widely separated beams are generally more robust against collisional decoherence than near-field interferometers. Cross-sections for scattering processes between large molecules and background gas are not very well known. So we can only extrapolate from our experiments with fullerenes, where we still see a measurable influence of the

background pressure on the collimation of the beam down to $p \sim 10^{-5}$ Pa. Deflections of the order of more than 30 nrad would already be detrimental in near-field interferometers for molecules or clusters around $m \sim 10^7$ amu. This shows the need for sophisticated vacuum techniques. Luckily, it has been demonstrated in positron trapping experiments [37] that it is possible to obtain a base pressure down to 10^{-15} Pa. This leaves enough room for the hope that collisions can be sufficiently suppressed – although at the expense of a substantial cryogenic effort.

24.3.7 Quasi-Static Interactions

In the preceding sections we have discussed the interaction with the environment through radiation. But also quasi-static interactions could betray the particle's position. Constant static field gradients shift the interference pattern by a constant amount. The magnitude of the field is thus encoded by and entangled with the position of the individual interference pattern on the screen. Decoherence would be induced by slowly and randomly varying field gradients which would shift the molecular phases in an uncontrolled way and therefore wash out the ensemble-averaged interference structure. The loss of information in this case is due to the inability of the experimentalist to correlate the instantaneous field values with the observed screen patterns. If he did this, the interference pattern could actually be completely restored.

This shows a general trend in the quantum physics of large systems: The number of degrees of freedom generally becomes so huge and the coupling to the environment so efficient that even a very enthusiastic and hard-working physicist will soon lose the details of all the available information. In the picture of decoherence, quantum mechanics is always valid but less and less visible, since the phase information somehow diffuses into the environment.

External fields could interact, for example, with the magnetic susceptibility or dipole moment, the electric polarizability or dipole moment or also with the mass of the molecule.

24.3.8 Magnetic Interactions

Isotopically pure $^{12}\text{C}_{60}$ in the electronic ground state is totally diamagnetic and has a small magnetic susceptibility. It has neither nuclear spin nor orbital angular momentum nor electronic spin. The interaction with magnetic fields in the lab can therefore be completely neglected. However, if we take into account the natural abundance of carbon (99% ^{12}C , 1% ^{13}C) we find [30] that in almost 50% of all fullerenes there is at least one ^{13}C which possesses one extra nuclear magneton. While now there is at least a handle for the interaction between the molecule and an external magnetic field, this handle and the separation of the arms of the interferometer is still too small to permit a significant phase shift in our experiment, even in the presence of very large magnetic field gradients. For larger objects with, for instance, a ferro-magnetic core this effect could become decisive.

24.3.9 Electric Interactions

The fullerenes have no permanent electric dipole moment but a sizable static polarizability of $\alpha_{\text{stat}} \sim 4\pi\epsilon_0 \times 80 \text{ \AA}^3$. Again, a significant phase difference between two paths in our experiment would require a setup especially designed for this purpose.⁵ Ordinary laboratory electric fields are too small by far to induce decoherence in buckyballs. Even for objects which possess a permanent electric dipole moment, such as large biomolecules⁶, we estimate that it should still be possible to control external stray fields well enough to avoid electrically induced decoherence in an interferometer.

24.3.10 Inertial Forces

Molecular de Broglie interferometers are very sensitive to inertial forces. The *gravitational phase shift* between two arms of an interferometer is due to the different energies of the molecule at different heights in the earth potential, while the rotation of an interferometer results in the quantum version of the Coriolis force, which is the *Sagnac effect*.⁷ In the diffraction experiment described above, both the gravitational and the rotational phase difference from the source to the screen are proportional to the mass of the quantum object. In a near-field interferometer – which is the more realistic device for coherence experiments with very large quantum objects – the sensitivity to inertial forces even increases quadratically with the mass. It turns out that for an earth-bound stationary experiment the gravitational phase shift is generally much more important than the Sagnac effect.

In principle, both effects can be zeroed for an appropriate choice of the orientation of the interferometer: The gravitational shift disappears if the surface vector of the interferometer is in line with the direction of the gravitational acceleration. Similarly, the rotational shift will disappear in an interferometer where the surface vector is orthogonal to the rotation axis. In three-dimensional space both directions can be adjusted independently. The earth's rotation and its gravitational field are sufficiently constant to allow the observation of high-contrast fringes even if the interferometer is somewhat misaligned. A constant phase shift would only displace the interference pattern. However, it is important to note that the phases introduced by the inertial forces are dispersive: different velocity classes will acquire different phase shifts, and therefore even a small misalignment may have a detrimental

⁵ One way to realize this is to implement an optical grating, i.e. a standing-wavelength field, which – due to its small wavelength – can generate important electric field gradients. This setup has actually been used to demonstrate interference at an optical grating for the first time for large molecules [38].

⁶ For hemoglobin the dipole moment amounts to 300 Debye (1 Debye = 3.33×10^{-30} Cm), roughly 200 times the value of water.

⁷ These two effects have been discussed by various authors. A good introduction can be found in [6].

effect. While in the case of our fullerenes an angle control to within a few milliradians is sufficient to maintain a good fringe visibility, the requirements on angular alignment and stability for an object the size of a virus is of the order of nanoradians. This is certainly at the extreme edge of currently available technologies.

24.3.11 Which-Way Information in Internal Clocks

As an alternative to entanglement with the environment, we may ask whether which-way information could be encoded in an internal clock.⁸ Suppose a molecule actually has a marker sitting on its surface and is prepared in a well-defined rotational state. One would then say that the marker will rotate with a given angular frequency and the number of turns as well as its phase can be taken as a measure of time. If now a molecule in a superposition of spatial wave packets passes two neighboring slits and proceeds to the left-hand first-order interference maximum, then – classically – one would expect the internal clock to show slightly different times. The wave passing the left-hand slit will arrive somewhat earlier than that taking the right-hand track. A constant time slip in the center of mass coordinates would simply shift the interference pattern. However, in the case described here the wave function is a product of the translational center of mass motion and the rotational evolution: $|\psi\rangle = |\psi_{\text{cm}}\rangle \otimes |\psi_{\text{rot}}\rangle$. The time scales for their evolution can be rather different. It may happen that the phase difference, $\Delta\phi_{\text{cm}} = k_{\text{dB}}\Delta L$, between the two interfering amplitudes of the center of mass motion is set to constructive interference, while the phase difference in the internal part, $\Delta\phi_{\text{rot}} = \omega_{\text{rot}}\tau$, is shifted and destructive. Actually the situation is even a bit more complicated since the molecular beam is in a thermal mixture of highly excited rotational states with an average angular momentum of $J \sim 150$, or an average angular frequency of about $\omega \sim 6 \times 10^{11} \text{ s}^{-1}$. But the question then is – even if we are neither able to prepare nor to read a well-defined initial or final rotational state: Which phase difference will be accumulated for the average rotational frequency due to the time difference related to the path-length difference, ΔL , towards the first-order interference maximum? If we take $\Delta L = \lambda_{\text{dB}} = 2 \text{ pm}$ and $v = 200 \text{ m/s}$ the time difference amounts to only $\tau \sim 10^{-14} \text{ s}$, yielding a phase shift of only $\Delta\phi_{\text{rot}} \sim 0.006 \text{ rad}$. Such a tiny phase difference is indeed very far from producing an orthogonal state. The internal clock is therefore unable to induce decoherence.

The relevance of internal clocks becomes even weaker for larger objects, since particles of larger mass and size possess a greater moment of inertia. Already at the same temperature they rotate at a lower frequency than their smaller counterparts. Interferometers working with even a reduced molecular temperature should therefore not be affected by internal clocks.

⁸ The question of internal clocks was brought to our attention by Chris Westbrook, IOTA, Orsay.

24.4 Conclusion

The sections above show that internal and external degrees of freedom are essentially decoupled and explain the persistence of interference in our fullerene experiments so far. A variety of novel decoherence experiments will be possible in a future extension of the experiment towards a large-area interferometer. A three-grating Talbot–Lau interferometer is being set up and will have a molecular beam separation of up to 1 μm . In this case the which-path information through a few thermal photons may become relevant.

Based on all the preceding arguments one can summarize that there is still a long way to go if one ever wants to find a fundamental limit for earth-based de Broglie interference experiments. But in order to actually see de Broglie interference with molecules in the range of $m \sim 1000 - 100\,000$ amu, the development of many novel and difficult techniques will be needed: The generation of intense, cold and neutral molecular beams is a big challenge, as is the detection with high spatial resolution of single or few macromolecules. Also, various coherent manipulation methods still have to be tested for such heavy particles.

However, the severest constraint in physics may actually be the limited power of our human imagination. Stretching the experimental limits of quantum mechanics is therefore always at the same time an effort to shift the limits of common belief. Thus, any such experiment is also a tribute to John Bell who – through his famous inequalities – gave us a criterion to test our classical prejudices against the reality of nature.

Acknowledgements

This work has been supported by the European TMR network, contract no. ERBFMRXCT960002, and by the Austrian Science Foundation (FWF), within the project F1505. O.N. acknowledges a grant by the Austrian Academy of Sciences. We acknowledge help in the setup of the experiment by Julia Petschinka.

References

1. For an overview and references, see the many other articles in this book
2. R.P. Feynman, R.B. Leighton, M.L. Sands: *The Feynman Lectures on physics, Vol. III: Quantum Mechanics* (Addison-Wesley, Reading, MA 1965)
3. W. Heisenberg: *Z. Phys.* **43**, 172 (1927)
4. C.J. Davisson, L.H. Germer: *Nature* **119**, 558 (1927);
G. Möllenstedt, C. Jönsson: *Z. Phys.* **155**, 472 (1959)
5. H. v. Halban Jr, P. Preiswerk: *C. R. Acad. Sci. Paris* **203**, 73 (1936)
6. H. Rauch, A. Werner: *Neutron interferometry: lessons in experimental quantum mechanics* (Oxford Univ. Press, London 2000)

7. I. Estermann, O. Stern: *Z. Phys.* **61**, 95 (1930)
8. M.H. Anderson, J.R. Ensher, M.R. Matthews, C.E. Wieman, E.A. Cornell: *Science* **269**, 198 (1995)
9. M. Arndt, O. Nairz, J. Voss-Andreae, C. Keller, G. van der Zouw, A. Zeilinger: *Nature* **401**, 680 (1999)
10. R. Mitzner, E.E.B. Campbell: *J. Chem. Phys.* **103**, 2445 (1995)
11. K. Hansen, E.E.B. Campbell: *Phys. Rev. E* **58**, 5477 (1998)
12. O. Nairz, M. Arndt, A. Zeilinger: *J. Mod. Opt.* **47**, 2811 (2000)
13. O. Nairz, M. Arndt, A. Zeilinger: *Phys. Rev. A* 032109 (2002)
14. E. Joos: In: *Decoherence and the Appearance of the Classical World in Quantum Theory*, ed. by D. Giulini et al. (Springer, Berlin, Heidelberg 1996)
15. M. Born, E. Wolf: *Principles of Optics*, 6th edn. (Pergamon Press, Oxford 1980) p. 510 & 514
16. T.A. Savas et al.: *J. Vac. Sci. Technol. B* **13**, 2732 (1995)
17. O. Nairz, M. Arndt, A. Zeilinger: *Am. J. Phys.* (in preparation)
18. M. Arndt, O. Nairz, J. Petschinka, A. Zeilinger: *C. R. Acad. Sci. Paris* **2**, série IV, 581 (2001)
19. R. Penrose: *Gen. Rel. Grav.* **28**, 581 (1996)
20. G.C. Ghirardi, A. Rimini, T. Weber: *Nuovo Cimento* **27**, 293 (1980)
21. W.H. Zurek: *Phys. Today* October, 36 (1991); W.H. Zurek: *Philos. Trans. R. Soc.* **356**, 1793 (1998)
22. E. Joos, H.D. Zeh: *Z. Phys. D.* **59**, 223 (1985)
23. N. Bohr (1927): In: *Albert Einstein, Philosopher-Scientist*, ed. by P. Schilpp (Tudor, New York 1949)
24. M.O. Scully, B.G. Englert, H. Walther: *Nature* **351**, 111 (1991)
25. S. Dürr, T. Nonn, G. Rempe: *Nature* **395**, 33 (1998)
26. J.F. Clauser, S. Li: *Phys. Rev. A* **50**, 2430 (1994)
27. T. Pfau, S. Spälter, C. Kurtsiefer, C.R. Ekstrom, J. Mlynek: *Phys. Rev. Lett.* **73**, 1223 (1994)
28. M.S. Chapman, T.D. Hammond, A. Lenef, J. Schmiedmayer, R.A. Rubenstein, E. Smith, D.E. Pritchard: *Phys. Rev. Lett.* **75**, 3783 (1995)
29. E. Kolodney, A. Budrevich, B. Tsipinyuk: *Phys. Rev. Lett.* **74**, 510 (1995)
30. M.S. Dresselhaus, G. Dresselhaus, P.C. Eklund: *Science of Fullerenes and Carbon Nanotubes* (Academic, New York 1996)
31. J.U. Andersen, E. Bonderup: *Eur. Phys. J. D* **11**, 435 (2000)
32. W.A. Chupka, C.E. Klotz: *Int. J. Mass. Spectrom. Ion. Proc.* **167/168**, 595 (1997)
33. O. Nairz, M. Arndt, A. Zeilinger: unpublished
34. G. Scoles (ed.): *Atomic and Molecular Beam Methods* (Oxford Univ. Press, Oxford 1988)
35. P. Heszler, J.O. Carlsson, P. Demirev: *J. Chem. Phys.* **107**, 10440 (1997)
36. C.E. Bohren, D.R. Huffman: *Absorption and Scattering of Light by Small Particles* (Wiley, New York 1983)
37. G. Gabrielse, X. Fei, L.A. Orozco, R.L. Tjoelker, J. Haas, H. Kalinowsky, T.A. Trainor, W. Kells: *Phys. Rev. Lett.* **65**, 1317 (1990)
38. O. Nairz, B. Brezger, M. Arndt, A. Zeilinger: *Phys. Rev. Lett.* **87**, 160401 (2001)

The original publication is available from
Springer-Verlag, Berlin, Heidelberg.

www.springeronline.com/3-540-42756-2